Influence of Activation Temperature on the Properties of Polyacrylonitrile-Based Activated Carbon Hollow Fiber

M.-C. YANG,[1] D.-G. YU[2]

[1] Department of Textile Engineering, National Taiwan University of Science and Technology, Taipei, Taiwan 106, Republic of China

[2] Department of Textile Engineering, Nanya Junior College, Chung-Li, Tao-Yuan, Taiwan 320, Republic of China

ABSTRACT: In this work, polyacrylonitrile hollow fiber was oxidized, carbonized, and activated by carbon dioxide into activated hollow carbon fiber. The effects of the activation temperature on the characteristics of the resulting activated hollow carbon fiber, including the mechanical properties, the surface area, and pore size distribution, were studied. The results show that by activating for 40 min at 800°C, the mechanical properties was better, the surface area was larger, and the pore size was distributed in three ranges. Higher activation temperature led to the decrease in the mechanical strength, the increase in the burn-off degree of the surface, the reduce of the portion of micropores, and the greatly broadening the pore size distribution. Lower activation temperature can only produce pleading on the surface of the fiber instead of open pores, due to the milder attack of CO_2. Therefore, the characteristics of the activated hollow carbon fiber can be controlled by the activation temperature. © 1998 John Wiley & Sons, Inc. J Appl Polym Sci 68: 1331–1336, 1998

Key words: activation temperature; activated carbon hollow fiber; polyacrylonitrile; mechanical properties

INTRODUCTION

There are many materials that can be used for manufacturing activated carbon. They can be classified according their origin.[1] Charcoal, saw dust, coconut shell, stones of many fruits, and other nut shells are of plant origin. Coal and asphalt are of mineral origin. The third class is from synthetic fiber, including regenerated cellulose, polyacrylonitrile (PAN), scrap tires, and other polymer scrap. The manufacturing process depends on the raw material. The activation is a process in which the gaseous activation agent reacts with the carbon source at a high temperature to develop the porous structure in the carbon matrix.[2] There are various types of pores in the activated carbon. Macropores have small specific surface area and are thus insignificant to adsorption; however, these pores control the access of adsorbate and also serves as the space for deposition. Mesopores provide channels for the adsorbate to the micropores from the macropores. Special methods are required to create mesopores, such as longer activation time, specific heating speed, and flow rate of activation agent. As reported in the literature, mesopore can function as capilary condensation, thus it is indispensable for the adsorption of liquid and gas. Micropores (< 1 nm) determine the adsorption capacity of the activated carbon. They have large specific surface areas and take the largest fraction of the adsorbed mass. Therefore, micropores are the major area of interest in the research of activated carbon.[3] Activated carbon are widely used in areas such as food, medicine, chemicals, defense, agriculture, water treatment, and environmental protection.[4–7]

Fibrous activated carbon is also known as active carbon fiber or is sometimes called carbon molecule sieve. The earliest fibrous activated carbon was made by bonding activated carbon powder to fibers.[8,9] These powders fell apart easily when used, and the adsorbing ability was less than conventional activated carbon powder. To improve these disadvantages, true fibrous activated carbon was made by direct oxidation, carbonization, and activation fibers of either natural or synthetic fibbers. This is known as the third generation of activated carbon.[10] In this laboratory, we have extended the activated carbon fiber to the form of asymmetric hollow fiber. These activated carbon hollow fibers (ACHF) have the following characteristics.

1. They are hollow and porous, which are useful for separating liquid or gaseous compositions, thus broadening their application.
2. They are self-supporting, therefore requiring small volumes for a large surface area, which shorten the operating time.
3. Their pore sizes can be controlled through the manufacturing conditions. A variety of product can thus be obtained.

In this work, we prepared PAN-based ACHF and investigated the influence of the activation temperature on the crystal size, mechanical properties, pore size distribution, and surface area of the ACHF.

EXPERIMENTAL

Preparation of PAN Hollow Fiber

The procedures were mentioned in our previous articles.[11-13] PAN hollow fibers used in this study were spun in this laboratory with a spinneret of inside diameter of 0.4 mm and outside diameter of 0.6 mm and with water as the coagulation liquid. The porous structure of these fibers is shown in Figure 1.

Preparation of ACHF

The PAN hollow fibers were first oxidized in air under a load of 0.1 g/denier at 230°C for 7 h. The oxidized hollow fibers were then carbonized at 1000°C for 40 min in nitrogen and were then heat-treated in carbon dioxide for 40 min at a temperature varying from 600 to 1000°C. Tension was not
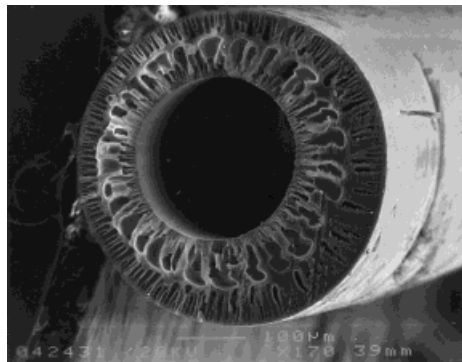

Figure 1 The cross section of original PAN hollow fiber.

applied to the fibers during carbonization and activation.

Characterization of ACHF

The mechanical properties of the hollow fibers and ACHF were determined using a tensile tester (Vibroskop, Lenzing AG) at a crosshead speed of 1 mm/min, and the testing gauge was 10 mm. In each case, about 25 specimens were tested and averaged. The crystal size of the fiber was determined using an X-ray diffractometer (Seintage DMS 2000) with Ni-filtered CuKα radiation. The crystal size (L_c) was estimated by the Scherrer equation,[14] as follows:

$$L_c = \frac{K\lambda}{B \cos \theta}$$

where λ is the wavelength of CuKα X-ray, B is the width at half-maximum intensity of the peak at $2\theta = 26°$, and the factor K is 0.89. The aromatization index (AI value) of the oxidized PAN fibers can be determined using the following X-ray method[15]:

$$AI = \frac{I_a}{I_a + I_p}$$

where I_a is the diffraction intensity of the aromatic structure at $2\theta = 26°$ and I_p is the diffraction intensity of the PAN crystal at $2\theta = 17°$. The cross sections and the surfaces of the fibers were examined with a scanning electron microscope (Cambridge S-360). The total surface area was measured using a Brunauer–Emmett–Teller (BET) porosimeter (Quantachrome Autosorb-6) and a mercury intrusion porosimeter (Quantachrome Autosorb-60) subject to pressure of 0–400 Mpa.

Table I   The Chemical Compositions and Properties of Precursor PAN-Based Hollow Fiber

Dope (Wt %)	M_w	M_w/M_n	Elemental Analysis			Crystal Size L_c (nm)	Tensile Strength (Gpa)	Modulus (Gpa)
			N%	C%	H%			
15%	307,000	2.0	20.13	60.15	6.47	0.88	0.47	16

RESULTS AND DISCUSSION

Effect of Activation Temperature on the Surface Structure

During the carbonization stage of carbon fiber, formation of carbon basal planes was due to the crosslinking reaction, and noncarbon elements evolved.[2] The mechanical strength was increased, but the surface area was reduced and hence was unsuitable for adsorption applications. By activating in CO_2 at high temperature, micropores suitable for adsorption purpose would appear on the surface and the internal of the carbon fiber.[2]

In this work, we prepare ACHF from PAN hollow fiber. The molecular weight and distribution, the composition, and the mechanical properties of the precursory PAN hollow fiber are listed in Table I. The characteristics of the resulting ACHF are listed in Table II. These ACHF were all oxidized at 230°C for 7 hr in air, carbonized at 1000°C for 40 min in N_2, and activated in CO_2 for 40 min at different temperatures. The resulting ACHFs show different structure, as those micrographs shown in Figure 2.

In Figures 2(a) and 3(a), we can see that by activating at 600°C, the shell of the fiber shrunk and appeared coarse with no formation of pores. We think that this is because during the carbonization at 1000°C, the carbon basal planes increasingly packed together and the activation at lower temperature promoted the formation of ordered graphitoidal layer structure. This would hinder the diffusion of CO_2 into the amorphous region to react with carbon. Therefore, the shell layer was not peeled off and only grained surface was resulted.

For the activation at 800°C, the shell layer was already peeled off after 30 min, and the ordered porous structure was exposed, as reported in our previous work.[11] In Figures 2(b) and 3(b), we can see that after activation for 40 min, pores of uniform size appear on the surface. We believe that this is because, after the sintering of the shell layer, the defects and the brim of the graphitoidal structure were gasified by CO_2 and those close pores were opened due to the vigorous attack of CO_2 and evolved into new pores.

As described by Bansal et al. that when activation at 1000°C, due to the diffusion of CO_2 into the defects of the molecular structure, vigorous reaction caused the tunneling of the skin layer and the pores, and larger pores were thus formed.[2] As shown in Figure 2(c) and 3(c), the pores became deeper and broader. Guigon et al.[16] suggested a theory for high strength carbon fiber, which indicates that the voids in the internal region of fiber are either connected or divided by amorphous carbon. Therefore, the activation at high temperature enables CO_2 to burn off the barrier amorphous carbon and, hence, makes the pores to be connected. This led to the attack of CO_2 deeper inside, and a coral-like structure was resulted.

### Effect of Activation Temperature on the Pore Size Distribution

Porous structure is the characteristics of activated carbon. The pore size distribution of ACHF is more diverse. As shown in Figure 3, the pore size distribution curve has peaks at 80 and 300 nm for the PAN precursor. After activation at 600°C, the peaks of the distribution shifted to 60 and 170 nm. This suggests that at lower tempera-

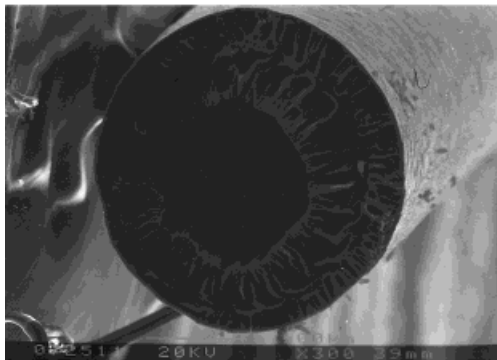**Table II   The Properties of PAN-Based Oxidized and Carbonized Hollow Fibers**

Sample	AI%	Tensile Strength (Gpa)	Modulus (Gpa)	Elongation (%)	L_c (nm)	Surface Area (m²/g)
Oxidized	60.2	0.41	6.3	2.89	—	—
Carbonized	—	1.43	83.0	1.03	1.2	158
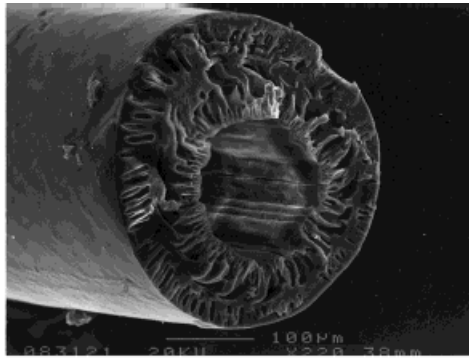
(a)
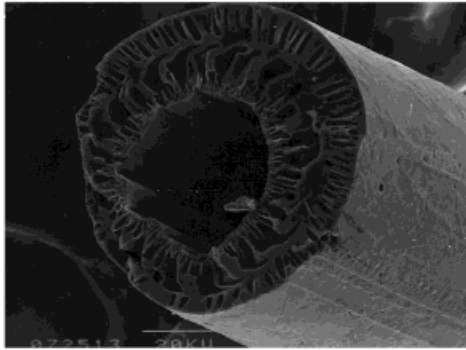
(b)

(c)

Figure 2 SEM micrographs of the cross section of activated carbon hollow fibers: (a) sample A; (b) sample B; (c) sample C.
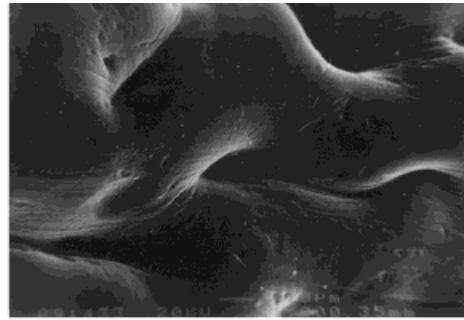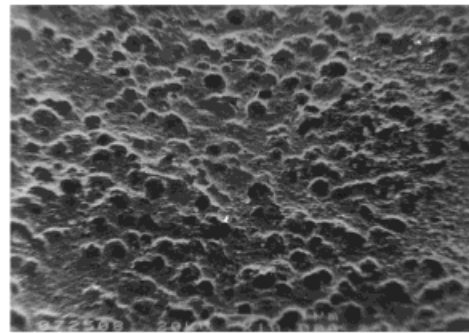

(a)

(b)

(c)

Figure 3 SEM micrographs of the surface of activated carbon hollow fibers: (a) sample A; (b) sample B; (c) sample C.
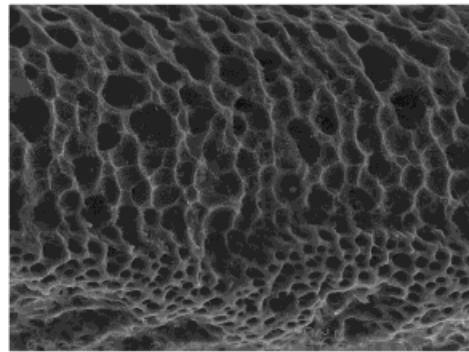
ture, the pores shrunk, and no micropores were formed. This is probably the continuing density of the stacking carbon basal plane structure. At 800°C, the peaks of the distribution curve shifted to 100 and 300 nm, and three new peaks appeared under 10 nm. When activation at 1000°C, the peaks of the distribution curve shifted to 123 and 280 nm, which were in the ranges of macro- and mesopore. This was the result of deepening and broadening of the attack of CO_2. This is in agreement with what Wigmans[17] indicated that new

pores will be created at lower activation temperature, and pore will be deepened at higher activation temperature.

Effect of Activation Temperature on the Mechanical Properties

We can see from Table II that after activating at 1000°C, the strength of ACHF was 1.43 Gpa, and the modulus was 83 Gpa. As shown in Table III, after activation, the strength and the modulus were decreased. The strength and modulus of

Table III   The Effect of Activation Temperature on the Properties of PAN-Based Activated Carbon Hollow Fibers

Sample	Activation Temperature (°C)	Tensile Strength (Gpa)	Modulus (Gpa)	Elongation (%)	Yield (%)	L_c (nm)
A	600	0.88	41.32	0.74	55	1.21
B	800	0.32	30.40	0.67	40	0.81
C	1000	0.17	18.15	0.45	26	0.63

sample C were dropped by 88 and 78%, respectively. The crystalline size was dropped by 50%. This is because CO_2 would activate first those non-graphitized carbon, hence leading to the deepening and broadening of pores at the fiber surface. For sample A, a lower temperature cannot effectively activate those non-graphitized carbon atoms, which only made the fiber to shrink and etched the surface. Therefore, the crystalline size and the mechanical properties were higher than samples B and C. As for sample B, the activation peeled the skin layer, and the closed pores were opened by CO_2, yet with no deepening and broadening.[18] The mechanical properties were still higher than sample C.

The carbon yield of sample A was 55% because the attacking of CO_2 only can occur at the surface. Sample C had only 26% of carbon yield. That is why its mechanical properties were the lowest. As reported by Grebennikov and Fridman,[19] micropores are formed for carbon yield below 50%, mixed porous structure resulted for a carbon yield of 50–70%, and macropores resulted for a carbon yield above 75%. This point was proven by Figure 4 and Table II.

Effect of Activation Temperature on the Surface Area

The surface area of ACHF was determined with the nitrogen adsorption method. As shown in Table IV, sample B has the largest surface area. This is because, at 800°C, the shell would shrink first, which would be easier for the attack of CO_2 to expose the pores underneath. Sample A has lower surface area because the CO_2 was unable to create new pores due to lower temperature. Sample C has the lowest surface area. Because pore size was enlarged due to the vigorous activation, the the surface area was thus reduced. Ko et al.[20] reported that the activation of solid carbon fiber consisted two simultaneous reactions: the condensation of dense layer, and the breaking of amorphous molecular chains. For sample C, the activation was

accelerated at high temperature, and the surface was not fully shrunk when the attack of CO_2 occurred. This made the pores deeper and broader.

CONCLUSION

Based upon the experimental results, we can conclude that at activation temperature higher than 1000°C, coral-like porous structure resulted in the depth because of the joining of pores. At low activation temperatures, CO_2 cannot diffuse deeper to cause activation in the depth of the fiber and can only etch the skin layer to form coarse surface. Therefore, at the suitable activation temperature, shrinkage would occur first on the surface. This would make the peeling easier by CO_2; hence, new pores would be created at the defects of the graphitoidal structure, and those existing pores would be deepened and broadened. The order of the occurrence of these two phenomena depends on the activation temperature.
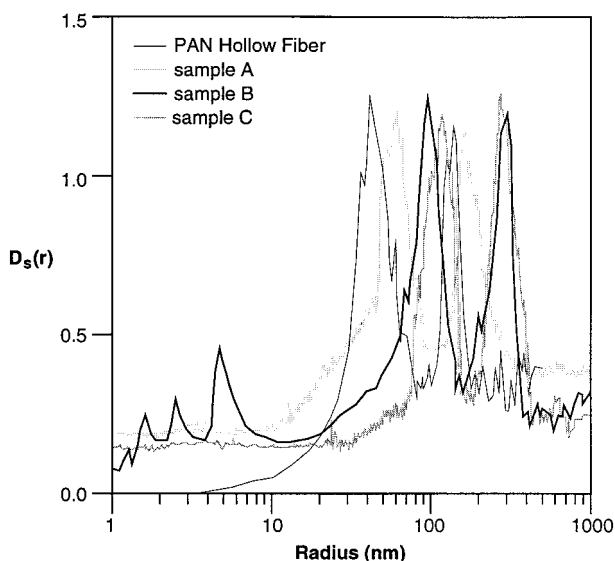

Figure 4   The pore size distribution of activated carbon hollow fiber.

Table IV   The Effect of Activation Temperature on the Chemical Compositions and Surface Area of PAN-Based Activated Carbon Hollow Fibers

Sample	Activation Temperature (°C)	Elemental Analysis				Surface Area (m²/g)
		N%	C%	H%	O%	
A	600	12.26	81.07	0.79	4.16	193
B	800	11.09	79.38	0.71	6.71	340
C	1000	10.36	74.96	0.66	5.87	179

REFERENCES

1. J. S. Mattson and H. B. Mark, *Activated Carbon,* Marcel Dekker, New York, 1971.
2. R. C. Bansal, J. B. Donnet, and F. Stoeckli, *Active Carbon,* Marcel Dekker, New York, 1988.
3. H. Jankowska, A. Swiatkowski, and J. Choma, *Active Carbon,* Ellis Horwood, New York, 1991.
4. P. Davina, *Carbon,* **28,** 565 (1990).
5. I. Mochida, T. Hirayama, S. Kawano, and H. Fujitsu, *Langmuir,* **8,** 2290 (1992).
6. S. Kisamori, K. Kuroda, S. Kawano, I. Mochida, Y. Matsumura, and M. Yoshikawa, *Energy Fuels,* **8,** 1337 (1994).
7. E. Richter, *Catal. Today,* **7,** 93 (1990).
8. G. P. Cobb and R. S. Braman, *Anal. Chem.,* **58,** 2213 (1986).
9. G. P. Cobb and R. S. Braman, *J. Air Waste Manage. Assoc.* **41,** 967 (1991).
10. M. Jaroniec and R. K. Gilpin, *Langmuir,* **7,** 2719 (1991).
11. M.-C. Yang and D.-G. Yu, *J. Appl. Polym. Sci.,* **58,** 185 (1995).
12. M.-C. Yang and D.-G. Yu, *Text. Res. J.,* **66,** 115 (1996).
13. M.-C. Yang and D.-G. Yu, *J. Appl. Polym. Sci.,* **59,** 1725 (1996).
14. B. D. Cullity, *Element of X-Ray Diffraction,* Addison-Wesley, Reading, MA, 1978.
15. T. Uchida, I. Shiniyama, Y. Ito, and K. Nukuda, *Proceedings of 10th Biennial Conference On Carbon,* Bethlehem, PA, 1971, p. 31.
16. M. Guigon, A. Oberlin, and G. Desarmat, *Fiber Sci. Tech.,* **20,** 177 (1984).
17. T. Wigmans, *Carbon,* **27,** 13 (1989).
18. B. Rand and H. March, *Carbon,* **9,** 79 (1971).
19. S. F. Grebennikov and L. I. Fridman, *Fiber Chem.,* **19,** 385 (1987).
20. T.-H. Ko, P. Chiranairadul, C.-K. Lu, and C.-H. Lin, *Carbon,* **30,** 647 (1992).